UCB-PTH-15/15

Composite Models for the 750 GeV Diphoton Excess

Keisuke Harigaya and Yasunori Nomura
Berkeley Center for Theoretical Physics, Department of Physics, University of California, Berkeley, CA 94720 and
Theoretical Physics Group, Lawrence Berkeley National Laboratory, Berkeley, CA 94720

We present composite models explaining the diphoton excess of mass around 750 GeV recently reported by the LHC experiments.

arXiv:1512.04850v3 [hep-ph] 12 May 2016

I. INTRODUCTION

Recently, the existence of a diphoton excess of mass around 750 GeV has been reported by both the ATLAS [1] and CMS [2] experiments at the LHC. The signals are still only 3.6 σ and 2.6 σ in the respective experiments, but if confirmed, this would indicate the long awaited discovery of new physics at the TeV scale.

Because of the Landau-Yang theorem [3], a particle decaying into two photons must have either spin 0, 2, or higher. Assuming spin 0, it is natural to postulate that the particle is a composite state of some strong dynamics around the TeV scale, since it would then not introduce any new hierarchy problem beyond that of the standard model Higgs boson, which may have an environmental understanding [4].

In fact, the relevance of strong dynamics is also suggested by the data. Suppose the diphoton resonance is a scalar field S of mass $m_S \simeq 750$ GeV, whose couplings to the gluon and photon are induced by the following interaction

$$\mathcal{L} = \lambda S Q \bar{Q}, \tag{1}$$

where λ is a coupling constant, and $(Q, \bar{Q})$ is a heavy vector-like fermion of mass m_Q charged under the standard model gauge group, $SU(3)_C \times SU(2)_L \times U(1)_Y$. Assuming that $(Q, \bar{Q})$ is an $SU(3)_C$ triplet and has charge q, its loop generates

$$\mathcal{L} \sim \frac{1}{24\pi^2} \frac{\lambda S}{m_Q} \left(\frac{1}{2} g_3^2 G^{a\mu\nu} G^a_{\mu\nu} + 3(qe)^2 F^{\mu\nu} F_{\mu\nu} \right), \tag{2}$$

where g_3 and e are the QCD and QED gauge couplings, respectively, and $G^a_{\mu\nu}$ and $F_{\mu\nu}$ are the corresponding field strengths. The production cross section of S through gluon fusion times the branching ratio into diphoton is then given by

$$\sigma_{pp\to S} B_{S\to AA} \simeq 0.2 \text{ fb} \times \lambda^2 \left(\frac{q}{2/3} \right)^4 \left(\frac{600 \text{ GeV}}{m_Q} \right)^2. \tag{3}$$

Here, we have normalized m_Q by its experimental lower bound [5]. (Note also that the decay of S into $Q\bar{Q}$ must be kinematically forbidden in order not to suppress the diphoton signal, giving $m_Q > m_S/2 \simeq 375$ GeV.) We find that to reproduce the observed excess, which requires $\sigma_{pp\to S} B_{S\to AA} \sim 10$ fb, the coupling λ must be rather large. This suggests the existence of strong dynamics behind the physics generating couplings between the resonance of interest and standard model gauge bosons.

	G_H	$SU(3)_C$	$U(1)_Y$
Q	$\square$	$\bar{\square}$	a
$\bar{Q}$	$\bar{\square}$	$\square$	$-a$

TABLE I. Charge assignment of a hidden "heavy" quark. Here, $a \neq 0$, and Q and $\bar{Q}$ are left-handed Weyl spinors.

Motivated by these considerations, in this paper we present models in which the observed diphoton excess arises from a composite particle of some hidden strong gauge interactions. We present a scenario in which the particle is a state around the dynamical scale (a hidden glueball or a hidden eta prime) as well as a scenario in which it is lighter (a hidden pion). We see that some of the models have possible tensions with diboson searches at 8 TeV, but others do not. In particular, we find that the model having the charge assignment consistent with $SU(5)$ grand unification has a parameter region in which the observed diphoton excess is reproduced without contradicting the other data. In general, the models described here yield multiple resonances in the TeV region, which may be observed in the future LHC data.

In the appendix, we present a general analysis of constraints from the 8 TeV data in the case that the scalar resonance is coupled to the standard model gauge fields only through dimension-5 operators.

II. HIDDEN GLUEBALL: MINIMAL MODEL

Consider a hidden gauge group G_H, with the dynamical scale (the mass scale of generic resonances) Λ. For simplicity, we take G_H to be $SU(N)$. We also introduce a vector-like hidden quark $(Q, \bar{Q})$ of mass m, whose charges under G_H and the standard model $SU(3)_C$ and $U(1)_Y$ are given in Table I. Here, Q and $\bar{Q}$ represent left-handed Weyl spinors.

For $m \gtrsim \Lambda$, the hidden quark can be regarded as a "heavy" quark (with respect to Λ), and the lightest hidden hadron will be a glueball s consisting of hidden sector gauge fields, of mass

$$m_s \sim \Lambda. \tag{4}$$

Due to the existence of $(Q, \bar{Q})$, we expect that this state

couples to the standard model gauge fields as

$$\mathcal{L} \sim -\frac{\Lambda^3}{4\pi m^4} s \left(\frac{g_3^2}{2} G^{a\mu\nu} G^a_{\mu\nu} + \frac{9a^2 g_1^2}{5} B^{\mu\nu} B_{\mu\nu} \right), \quad (5)$$

where $a = 1, \cdots, 8$ is the $SU(3)_C$ adjoint index, and g_3 and g_1 are the $SU(3)_C$ and $U(1)_Y$ gauge couplings, respectively.[1] Here and below, we count possible factors of 4π using naive dimensional analysis [6].

The hidden glueball state s can be produced by gluon fusion (among others) and decay into diphoton with the branching ratio

$$B_{s\to\gamma\gamma} = \frac{81a^4}{50} \frac{\cos^4\theta_W g_1^4}{8 g_3^4} \simeq 0.033\, a^4, \quad (6)$$

where θ_W is the Weinberg angle. The production cross section of s through Eq. (5) at 13 TeV pp collisions can be estimated (after multiplying the diphoton branching ratio) as

$$\sigma_{pp\to s} B_{s\to\gamma\gamma} \sim 10 \text{ fb} \times a^4 \left(\frac{3.5 \text{ TeV}}{m^4/\Lambda^3} \right)^2, \quad (7)$$

where we have used NNPDF 3.0 [7] for the parton distribution function. We thus find that

$$\Lambda \sim 700 \text{ GeV}, \qquad m \sim 1 \text{ TeV}, \quad (8)$$

give m_s and $\sigma_{pp\to s} B_{s\to\gamma\gamma}$ roughly consistent with the excess in the 13 TeV data.

The model is subject to constraints from analogous high-mass diboson resonance searches in the 8 TeV data. Assuming that the production occurs through interactions in Eq. (5), the ratio of the s production cross sections at 8 TeV and 13 TeV is

$$\frac{\sigma_{pp\to s}|_{8\,\text{TeV}}}{\sigma_{pp\to s}|_{13\,\text{TeV}}} \simeq 0.21, \quad (9)$$

for $m_s = 750$ GeV. This gives $\sigma_{pp\to s} B_{s\to\gamma\gamma}$ close to the upper limit from the 8 TeV data [8]. The model also gives definite predictions for the relative branching ratios between $s \to \gamma\gamma, ZZ$, and $Z\gamma$

$$\frac{B_{s\to ZZ}}{B_{s\to\gamma\gamma}} = \tan^4\theta_W \simeq 0.09, \quad (10)$$

$$\frac{B_{s\to Z\gamma}}{B_{s\to\gamma\gamma}} = 2\tan^2\theta_W \simeq 0.6, \quad (11)$$

where we have ignored the phase space factors. With Eq. (9), we thus obtain

$$\sigma \times B|_{Z\gamma,\,8\,\text{TeV}} \simeq 1.3 \text{ fb} \left(\frac{\sigma \times B|_{\gamma\gamma,\,13\,\text{TeV}}}{10 \text{ fb}} \right). \quad (12)$$

[1] Throughout the paper, we adopt the hypercharge normalization such that the standard model fermions have $(q, \bar{u}, \bar{d}, l, \bar{e}) = (1/6, -2/3, 1/3, -1/2, 1)$, and g_1 is in the $SU(5)$ normalization.

	G_H	$SU(3)_C$	$U(1)_Y$	$U(1)_A$
Q_1	$\square$	$\bar{\square}$	a	$1/3$
Q_2	$\square$	$\mathbf{1}$	b	-1
$\bar{Q}_1$	$\bar{\square}$	$\square$	$-a$	$1/3$
$\bar{Q}_2$	$\bar{\square}$	$\mathbf{1}$	$-b$	-1

TABLE II. Charge assignment of hidden "light" quarks. Here, $a^2 \neq b^2$, and $Q_{1,2}$ and $\bar{Q}_{1,2}$ are left-handed Weyl spinors.

This is consistent with the upper limit from the 8 TeV data [9].

We note that the precise value of $\sigma \times B|_{8\,\text{TeV}}$ depends on the details of s production, which we have assumed here to occur only through Eq. (5). (For an analysis of constraints from the 8 TeV data for general dimension-5 couplings between s and the standard model gauge fields, see the appendix.) The assumption of gluon fusion dominated production, however, may not be valid in some cases. For example, depending on the values of m and Λ, production of heavy resonances that are composed of Q and $\bar{Q}$ and decay into s may give comparable contributions to the production of single s through the gluon fusion. With this production mechanism, the production rates of s in 8 TeV and 13 TeV pp collisions will differ more, relaxing the constraints from the 8 TeV data. The production mechanisms can be differentiated experimentally, e.g., through the transverse momentum distribution of photons. Detailed analyses of this issue are warranted.

Limits from other diboson decays of s, i.e. to gg and ZZ, are weaker.

III. HIDDEN PION: MINIMAL MODEL

We now consider a model in which the 750 GeV resonance is a hidden "pion," instead of the hidden glueball. A virtue of this model is that we need to rely less on the dynamical assumption about the hidden sector. As before, we take the hidden gauge group G_H to be $SU(N)$, but now we take the hidden quarks to have charges in Table II and mass terms

$$\mathcal{L} = -m_1 Q_1 \bar{Q}_1 - m_2 Q_2 \bar{Q}_2 + \text{h.c.}, \quad (13)$$

where we take $m_{1,2} > 0$ without loss of generality. We assume that these masses are sufficiently smaller than the dynamical scale, $m_{1,2} \ll \Lambda$, so that $Q_{1,2}$ and $\bar{Q}_{1,2}$ can be regarded as hidden "light" quarks.

A. Hidden Pion Dynamics

The strong G_H dynamics makes the hidden quarks condensate

$$\langle Q_1 \bar{Q}_1 \rangle \approx \langle Q_2 \bar{Q}_2 \rangle \equiv \langle Q\bar{Q} \rangle \approx \frac{1}{16\pi^2} \Lambda^3. \quad (14)$$

These condensations do not break the standard model $SU(3)_C$ or $U(1)_Y$, since the hidden quark quantum numbers under these gauge groups are vector-like with respect to G_H [10]. The spectrum below Λ then consists of hidden pions, arising from spontaneous breaking of approximate $SU(4)_A$ axial flavor symmetry:

$$\begin{array}{ll} \psi \sim Q_1\bar{Q}_1 & (\mathbf{Adj}, 0), \\ \chi \sim Q_1\bar{Q}_2 & (\Box, a-b), \\ \phi \sim Q_1\bar{Q}_1 - Q_2\bar{Q}_2 & (\mathbf{1}, 0), \end{array} \tag{15}$$

where ψ and ϕ are real scalars while χ is a complex scalar. The quantum numbers in the rightmost column represent those under $SU(3)_C \times U(1)_Y$. The masses of these particles are given by [11]

$$m_\psi^2 = 2m_1\frac{\langle Q\bar{Q}\rangle}{f^2} + 3\Delta_C, \tag{16}$$

$$m_\chi^2 = (m_1+m_2)\frac{\langle Q\bar{Q}\rangle}{f^2} + \frac{4}{3}\Delta_C + \frac{3(a-b)^2}{5}\Delta_Y, \tag{17}$$

$$m_\phi^2 = \frac{m_1+3m_2}{2}\frac{\langle Q\bar{Q}\rangle}{f^2}. \tag{18}$$

Here, f is the decay constant, given by

$$f \approx \frac{1}{4\pi}\Lambda, \tag{19}$$

and Δ_C and Δ_Y are contributions from $SU(3)_C$ and $U(1)_Y$ gauge loops, of order

$$\Delta_C \approx \frac{g_3^2}{16\pi^2}\Lambda^2, \qquad \Delta_Y \approx \frac{g_1^2}{16\pi^2}\Lambda^2. \tag{20}$$

We assume that ϕ is the lightest hidden pion, which can be ensured by making m_2 smaller with respect to m_1. This particle is the pseudo Nambu-Goldstone boson of $U(1)_A \subset SU(4)_A$, whose charges are given in Table II. The couplings of ϕ to the standard model gauge fields are determined by the $U(1)_A$-$SU(3)_C^2$ and $U(1)_A$-$U(1)_Y^2$ anomalies and are given by[2]

$$\mathcal{L} = -\frac{Ng_3^2}{32\sqrt{6}\pi^2 f}\phi G^{a\mu\nu}\tilde{G}^a_{\mu\nu} - \frac{9(a^2-b^2)Ng_1^2}{80\sqrt{6}\pi^2 f}\phi B^{\mu\nu}\tilde{B}_{\mu\nu}, \tag{21}$$

where $\tilde{G}^a_{\mu\nu} \equiv \epsilon_{\mu\nu\rho\sigma}G^{a\rho\sigma}/2$ and similarly for $\tilde{B}_{\mu\nu}$. Therefore, ϕ can be produced by gluon fusion and decay into diphoton with a significant branching ratio. Similar anomaly induced couplings also exist between ψ and $G^{\mu\nu}\tilde{G}_{\mu\nu}$ and for $a \neq 0$ between ψ and $G^{\mu\nu}\tilde{B}_{\mu\nu} = B^{\mu\nu}\tilde{G}_{\mu\nu}$, but not for other combinations of hidden pions and standard model gauge bosons.

[2] The definition of our decay constant, f, is a factor of 2 smaller than that in Ref. [11]: $f = F/2$.

B. Parameter Region and Constraints

Assuming that ϕ production occurs only through interactions in Eq. (21), the production cross section at 13 TeV pp collisions is given by

$$\sigma_{pp\to\phi} \simeq 270 \text{ fb}\left(\frac{N}{5}\frac{600 \text{ GeV}}{f}\right)^2. \tag{22}$$

From Eq. (21), we find that

$$B_{\phi\to\gamma\gamma} = \frac{81(a^2-b^2)^2\cos^4\theta_W g_1^4}{50 g_3^4}, \tag{23}$$

so we obtain

$$\sigma_{pp\to\phi}B_{\phi\to\gamma\gamma} \simeq 8.9 \text{ fb}\left(\frac{N(a^2-b^2)}{5}\frac{600 \text{ GeV}}{f}\right)^2. \tag{24}$$

This determines the decay constant as

$$f \simeq 570 \text{ GeV}\,\frac{N(a^2-b^2)}{5}\sqrt{\frac{10 \text{ fb}}{\sigma_{pp\to\phi}B_{\phi\to\gamma\gamma}}}. \tag{25}$$

We then obtain from Eq. (18, 19)

$$\frac{m_1+3m_2}{4} \approx \frac{m_\phi^2}{8\pi f} \simeq 40 \text{ GeV}\left(\frac{570 \text{ GeV}}{f}\right), \tag{26}$$

where we have used $m_\phi = 750$ GeV in the last expression. Note, however, that this equation has an $O(1)$ uncertainty arising from an unknown coefficient in Eq. (19).

We thus find that the model reproduces the observed diphoton excess for

$$f \sim 600 \text{ GeV}, \qquad m_{1,2} \sim 40 \text{ GeV}. \tag{27}$$

Since the relative branching ratios between $\phi \to \gamma\gamma, ZZ$, and $Z\gamma$ are the same as those of s in the previous model, Eqs. (10, 11), the present model is subject to the same constraints from searches of high-mass diboson resonances in the 8 TeV data.

Other constraints on the model may come from the existence of heavier hidden pions, ψ and χ. In particular, without higher dimension operators coupling the hidden and standard model sectors and suppressed by a scale not far above Λ, the χ particle is stable at collider timescales. Once produced, it hadronizes picking up a light quark of the standard model. For $|a-b| = 2/3$ and $1/3$, for example, this particle appears as heavy stable top and bottom scalar quarks, respectively. The lower bounds on the masses of such particles are about 800–900 GeV [12]. We expect that m_χ satisfies this bound for $m_1 \sim m_2$ due to the contribution from $SU(3)_C$ gauge loop, Δ_C, but if not, we can always make $m_\chi > 900$ GeV keeping $m_\phi = 750$ GeV by making m_2 smaller relative to m_1.

	G_H	$SU(3)_C$	$SU(2)_L$	$U(1)_Y$	$U(1)_A$
Q_1	$\square$	$\bar{\square}$	$\mathbf{1}$	$1/3$	$1/3$
Q_2	$\square$	$\mathbf{1}$	$\square$	$-1/2$	$-1/2$
$\bar{Q}_1$	$\bar{\square}$	$\square$	$\mathbf{1}$	$-1/3$	$1/3$
$\bar{Q}_2$	$\bar{\square}$	$\mathbf{1}$	$\square$	$1/2$	$-1/2$

TABLE III. Charge assignment of hidden quarks consistent with grand unification.

C. Variations—Hidden Eta Prime

It is interesting to consider a parameter region of the model with $m_2 \ll \Lambda \ll m_1$. In this case, we expect that the lightest hidden hadron is the hidden η' particle of mass $\sim \Lambda$, consisting of $Q_2\bar{Q}_2$. The production of this particle occurs through that of heavy resonances involving Q_1 and $\bar{Q}_1$, which then decay into two or more hidden η'. (The decay of the lightest heavy resonance into an even number of η' would require parity violation, which can be provided by the θ term of G_H, $\theta_H \neq 0$.) This makes the production cross sections at 8 TeV and 13 TeV more hierarchical than in Eq. (9), alleviating/eliminating possible tensions with the 8 TeV data. The decay of the hidden η' is mostly into two electroweak gauge bosons, without having a significant branching into two gluons.

We mention that this model may exhibit an intriguing set of signals if $\theta_H = 0$. In this case, a heavy "η" consisting of $Q_1\bar{Q}_1$, which we call $\tilde{\eta}$, cannot decay into η' because of parity conservation (unless the three η' mode is kinematically open) and hence decays into gg and $\gamma\gamma$. On the other hand, a heavy "ρ," having $J^{PC} = 1^{--}$, decays into γ and η', which subsequently decays as $\eta' \to \gamma\gamma$. Therefore, by choosing $m_{\eta'} = 750$ GeV and $m_{\tilde{\eta}} \simeq 1.6$ TeV we may also be able to accommodate the second, (much) weaker diphoton excess seen around 1.6 TeV in the ATLAS data [1]. To be conclusive, however, a more detailed analysis is needed.

IV. MODELS CONSISTENT WITH UNIFICATION

We finally discuss a model in which the charge assignment of the hidden quarks is consistent with $SU(5)$ grand unification [13]. We take the hidden quarks to be a vector-like fermion in the bifundamental representation of G_H and $SU(5)$, as shown in Table III, and write down their mass terms as in Eq. (13). Depending on the relative sizes of Λ and $m_{1,2}$, this model realizes either the hidden glueball or hidden pion scenario.

A. Hidden Glueball

For $m_{1,2} \gtrsim \Lambda$, the lightest hidden hadron is the hidden glueball s, which interacts with the standard model gauge fields as

$$\mathcal{L} \sim -\frac{\Lambda^3}{4\pi m_1^4} s \left(\frac{g_3^2}{2} G^{a\mu\nu} G^a_{\mu\nu} + \frac{g_1^2}{5} B^{\mu\nu} B_{\mu\nu} \right) - \frac{\Lambda^3}{4\pi m_2^4} s \left(\frac{g_2^2}{2} W^{b\mu\nu} W^b_{\mu\nu} + \frac{3g_1^2}{10} B^{\mu\nu} B_{\mu\nu} \right), \quad (28)$$

where $b = 1, 2, 3$ is the $SU(2)_L$ adjoint index, and g_2 is the $SU(2)_L$ gauge coupling. For $m_1 \ll m_2$, the phenomenology is essentially the same as the non-unified model before. For $m_2 \ll m_1$, on the other hand, the production of s occurs through that of heavy resonances involving Q_1 and $\bar{Q}_1$. (In order for the lightest heavy resonance to decay into two s, we need to break parity by $\theta_H \neq 0$.) The produced s decays mostly into electroweak gauge bosons, with the relative branching ratios

$$R^s_{WW} \simeq 9, \qquad R^s_{ZZ} \simeq 10, \qquad R^s_{Z\gamma} \simeq 0.7, \quad (29)$$

where $R^s_{XY} \equiv B_{s\to XY}/B_{s\to\gamma\gamma}$. By choosing $m_s = 750$ GeV, we can explain the observed diphoton excess.

B. Hidden Pion

For $m_{1,2} \ll \Lambda$, the low energy spectrum consists of hidden pions with the following standard model quantum numbers:

$$\begin{array}{ll} \psi(\mathbf{Adj}, \mathbf{1}, 0), & \chi(\square, \square, -5/6), \\ \varphi(\mathbf{1}, \mathbf{Adj}, 0), & \phi(\mathbf{1}, \mathbf{1}, 0), \end{array} \quad (30)$$

where ψ, φ, and ϕ are real scalars while χ is a complex scalar. In this case, we can make ϕ the lightest hidden pion and identify it with the observed 750 GeV resonance. The production and decay of this particle are both controlled by the anomaly induced couplings

$$\mathcal{L} = -\frac{N g_3^2}{16\sqrt{15}\pi^2 f} \phi G^{a\mu\nu} \tilde{G}^a_{\mu\nu} + \frac{3N g_2^2}{32\sqrt{15}\pi^2 f} \phi W^{b\mu\nu} \tilde{W}^b_{\mu\nu} + \frac{N g_1^2}{32\sqrt{15}\pi^2 f} \phi B^{\mu\nu} \tilde{B}_{\mu\nu}, \quad (31)$$

giving the relation in Eq. (9) and

$$\frac{B_{\phi\to Z\gamma}}{B_{\phi\to\gamma\gamma}} = 2 \left(\frac{9 - 5\tan^2\theta_W}{14\tan\theta_W} \right)^2 \simeq 2. \quad (32)$$

This leads to

$$\sigma \times B|_{Z\gamma,\,8\,\mathrm{TeV}} \simeq 4.0\ \mathrm{fb} \left(\frac{\sigma \times B|_{\gamma\gamma,\,13\,\mathrm{TeV}}}{10\ \mathrm{fb}} \right), \quad (33)$$

yielding a possible tension with the 8 TeV data [9].

Another interesting region is the one in which φ is the lightest, or only, hidden pion. A simple realization of this scenario occurs if

$$m_2 < \Lambda \lesssim m_1. \quad (34)$$

In this case, the spectrum below Λ consists only of

$$\varphi \sim Q_2 \bar{Q}_2 \quad (\mathbf{1}, \mathbf{Adj}, 0), \tag{35}$$

of mass

$$m_\varphi^2 = 2m_2 \frac{\langle Q\bar{Q}\rangle}{f^2} + 2\Delta_L, \tag{36}$$

where $\Delta_L \approx (g_2^2/16\pi^2)\Lambda^2$ represents the contribution from $SU(2)_L$ gauge loop. The only anomaly induced coupling between this particle and the standard model gauge fields is

$$\mathcal{L} = \frac{3Ng_2g_1}{16\sqrt{15}\pi^2 f}\varphi^b W^{b\mu\nu}\tilde{B}_{\mu\nu}, \tag{37}$$

so its production must occur through that of heavy resonances involving Q_1 and $\bar{Q}_1$ which decay into two or more φ (with two φ from the lightest heavy resonance needing $\theta_H \neq 0$). This, therefore, does not lead to the (potentially problematic) relation in Eq. (9).

The probability of producing each of the three isospin components of φ—φ^0 and $\varphi^\pm$—is 1/3. The produced φ^0 decays into ZZ, $\gamma\gamma$, and $Z\gamma$ with the branching ratios

$$\begin{aligned} B_{\varphi^0\to ZZ} &= B_{\varphi^0\to\gamma\gamma} = 2\sin^2\theta_W\cos^2\theta_W \simeq 0.35, \\ B_{\varphi^0\to Z\gamma} &= \left(\cos^2\theta_W - \sin^2\theta_W\right)^2 \simeq 0.30, \end{aligned} \tag{38}$$

while $\varphi^\pm$ into WZ and $W\gamma$ with $\sin^2\theta_W \simeq 0.23$ and $\cos^2\theta_W \simeq 0.77$, respectively. Thus, for each production of the heavy resonance, the probabilities of having $\gamma\gamma$ and $Z\gamma$ in the final state are

$$P_{\gamma\gamma} = \frac{2}{3}B_{\varphi^0\to\gamma\gamma} - \frac{1}{9}B_{\varphi^0\to\gamma\gamma}^2 \simeq 0.22, \tag{39}$$

$$P_{Z\gamma} = \frac{2}{3}B_{\varphi^0\to Z\gamma} - \frac{1}{9}B_{\varphi^0\to Z\gamma}^2 \simeq 0.19, \tag{40}$$

where we have assumed that each heavy resonance leads to two φ. This implies that the production cross section of heavy resonances of order

$$\sigma \sim \frac{10\text{ fb}}{P_{\gamma\gamma}} \simeq 45\text{ fb}, \tag{41}$$

allows for explaining the diphoton excess.

Estimating the production cross section of heavy resonances by that of a heavy vector-like quark of mass $\sim$ TeV, we obtain [14]

$$\sigma \sim 60\text{ fb}\left(\frac{N}{2}\right). \tag{42}$$

We thus expect that the model yields the observed level of the diphoton excess for

$$m_1 \sim 1\text{ TeV}, \qquad N \sim O(1). \tag{43}$$

Indeed, with this choice of m_1, the ratio of the production cross sections at 8 and 13 TeV is

$$\frac{\sigma|_{8\,\text{TeV}}}{\sigma|_{13\,\text{TeV}}} \sim 0.05\text{–}0.1, \tag{44}$$

which is about a factor of 2 smaller than in Eq. (9). Together with

$$\frac{P_{Z\gamma}}{P_{\gamma\gamma}} \simeq 0.85, \tag{45}$$

we find that the upper limit on the $Z\gamma$ mode from the 8 TeV search can be safely evaded. The limits from other diboson modes, WZ and $W\gamma$ from $\varphi^\pm$ and ZZ and $\gamma\gamma$ from φ^0, do not constrain the model further.

Taking $m_1 \sim 1$ TeV also allows for avoiding bounds [12] from possible particles which are stable at collider timescales, e.g. states analogous to χ in Eq. (30). The mass of the Q_2 hidden quark is determined by the condition $m_\varphi = 750$ GeV as

$$m_2 \sim 300\text{ GeV}\,\frac{1\text{ TeV}}{\Lambda}, \tag{46}$$

through Eq. (36). We thus find that the model reproduces the observed diphoton excess while being consistent with the other experimental data, with the choice of parameters

$$m_1 \sim \Lambda \sim 1\text{ TeV}, \qquad m_2 \sim 300\text{ GeV}, \tag{47}$$

for $N \sim O(1)$. Note that the value of Λ can be somewhat smaller if it is compensated by the correspondingly larger value of m_2 to keep $m_\varphi = 750$ GeV, see Eq. (46).

V. DISCUSSION

In this paper, we have presented models in which the reported diphoton excess of mass around 750 GeV is explained by composite states of hidden strong gauge interactions. The models are technically natural—i.e. do not introduce any new hierarchy problem beyond that of the standard model Higgs boson—and are consistent with the other experimental data (although some of them may have potential tensions with the 8 TeV data). In particular, we have constructed a simple model consistent with $SU(5)$ grand unification, in which the hidden quarks are in the bifundamental representation of G_H and $SU(5)$. This model is consistent with the data and preserves gauge coupling unification at the level of the standard model (which is significant; see discussion in Ref. [15], for example). Interestingly, some of the parameter regions have the ratio of the hidden quark masses, $m_1/m_2 \sim 3$, which is roughly consistent with the effect of renormalization group evolution between the TeV and unification scales.

Models presented here require a coincidence of scales between the dynamical scale, Λ, and the masses of hidden quarks, m. This can be explained, for example, if the G_H gauge theory is in the strongly coupled conformal window above TeV and deviates from it in the infrared due to the effect of the hidden quark masses that originate from a common scale. The conformal nature of the dynamics may also help alleviating potential cosmological

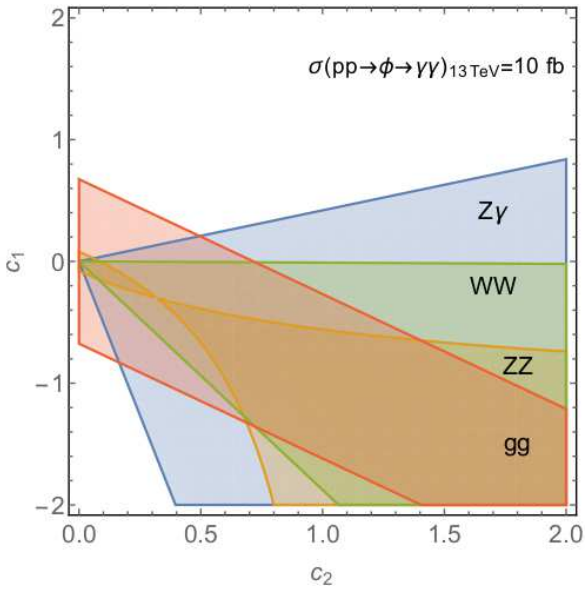


FIG. 1. Constraints on the coefficients of the dimension-5 operators, c_2 and c_1. The shaded regions are excluded by the searches in the 8 TeV data.

problems associated with stable particles in the G_H sector by enhancing their couplings to the standard model particles.

It is interesting that a simple structure described here—new G_H gauge interactions with vector-like matter charged under both G_H and the standard model gauge groups—explains the observed excess(es) while still consistent with the other experimental data. If the theory presented here is true, then the LHC Run 2 would see a plethora of new phenomena arising from the new strong gauge interactions.

Note added: After this paper was submitted to arXiv, we became aware of the works in Ref. [16] which discuss similar theories. These works focus mostly on phenomenology of spin-1 resonant production of hidden hadron pairs.

ACKNOWLEDGMENTS

We would like to thank Lawrence Hall, Tongyan Lin, Hou Keong Lou, Michele Papucci, Alex Pomarol, Surjeet Rajendran, and Kathryn Zurek for discussions. This work was supported in part by the Director, Office of Science, Office of High Energy and Nuclear Physics, of the U.S. Department of Energy under Contract DE-AC02-05CH11231, by the National Science Foundation under grants PHY-1316783 and PHY-1521446, and by MEXT KAKENHI Grant Number 15H05895.

Appendix A: General Dimension-5 Operators

In this appendix, we analyze consistency between the diphoton signal at 13 TeV and diboson searches at 8 TeV, assuming general dimension-5 operators coupling a singlet scalar ϕ with the standard model gauge fields:

$$\mathcal{L} = \frac{\phi}{4\pi\Lambda}\left(g_3^2 G^{a\mu\nu}\tilde{G}^a_{\mu\nu} + c_2 g_2^2 W^{b\mu\nu}\tilde{W}^b_{\mu\nu} + \frac{3c_1}{5} g_1^2 B^{\mu\nu}\tilde{B}_{\mu\nu}\right). \tag{A1}$$

(Our analysis applies if we replace $\tilde{G}^a_{\mu\nu}$ with $G^a_{\mu\nu}$, and similarly for $\tilde{W}^b_{\mu\nu}$ and $\tilde{B}_{\mu\nu}$.) We assume that the scalar ϕ is produced via gluon fusion and decays into standard model gauge bosons.

The constraint on each decay mode at the 8 TeV LHC is given by[3]

$$\begin{array}{ll} \sigma_{pp\to\phi} B_{\phi\to\gamma\gamma} < 2 \text{ fb} & [8] \\ \sigma_{pp\to\phi} B_{\phi\to Z\gamma} < 5 \text{ fb} & [9] \\ \sigma_{pp\to\phi} B_{\phi\to ZZ} < 30 \text{ fb} & [17] \\ \sigma_{pp\to\phi} B_{\phi\to W^+W^-} < 80 \text{ fb} & [17] \\ \sigma_{pp\to\phi} B_{\phi\to gg} < 5000 \text{ fb} & [18] \end{array} \tag{A2}$$

In Fig 1, we show the constraints on c_2 and c_1 from the 8 TeV data, choosing Λ such that the diphoton signal of 10 fb is obtained at 13 TeV. We find that the limits from the $Z\gamma$ and ZZ modes are constraining. However, there is still a parameter region in which the observed diphoton excess at 13 TeV is consistent with the limits from the 8 TeV searches.

[1] M. Kado, "ATLAS results" Talk at ATLAS and CMS physics results from Run 2, CERN, Switzerland, December 15 (2015); ATLAS Collaboration, "Search for new physics decaying to two photons," ATLAS-CONF-2015-081.

[2] J. Olsen, "CMS results," Talk at ATLAS and CMS physics results from Run 2, CERN, Switzerland, December 15 (2015); CMS Collaboration, "Search for new physics in high mass diphoton events in proton-proton collisions at 13 TeV," CMS-PAS-EXO-15-004.

[3] L. D. Landau, "On the angular momentum of a system of two photons," Dokl. Akad. Nauk Ser. Fiz. **60**, 207 (1948); C. N. Yang, "Selection rules for the dematerialization of a particle into two photons," Phys. Rev. **77**, 242 (1950).

[4] V. Agrawal, S. M. Barr, J. F. Donoghue and D. Seckel, "The anthropic principle and the mass scale of the standard model," Phys. Rev. D **57**, 5480 (1998) [hep-ph/9707380].

[5] G. Aad *et al.* [ATLAS Collaboration], "Search for pair production of a new heavy quark that decays into a W

[3] To obtain the constraint from the gg channel, we assume that the acceptance of the signal is 0.6, which is the case for an octet scalar decaying to two gluons.

boson and a light quark in pp collisions at $\sqrt{s} = 8$ TeV with the ATLAS detector," arXiv:1509.04261 [hep-ex].

[6] A. Manohar and H. Georgi, "Chiral quarks and the non-relativistic quark model," Nucl. Phys. B **234**, 189 (1984).

[7] R. D. Ball *et al.* [NNPDF Collaboration], "Parton distributions for the LHC Run II," JHEP **04**, 040 (2015) [arXiv:1410.8849 [hep-ph]].

[8] G. Aad *et al.* [ATLAS Collaboration], "Search for high-mass diphoton resonances in pp collisions at $\sqrt{s} = 8$ TeV with the ATLAS detector," Phys. Rev. D **92**, 032004 (2015) [arXiv:1504.05511 [hep-ex]]; CMS Collaboration, "Search for high-mass diphoton resonances in pp collisions at $\sqrt{s} = 8$ TeV with the CMS detector," CMS-PAS-EXO-12-045.

[9] G. Aad *et al.* [ATLAS Collaboration], "Search for new resonances in $W\gamma$ and $Z\gamma$ final states in pp collisions at $\sqrt{s} = 8$ TeV with the ATLAS detector," Phys. Lett. B **738**, 428 (2014) [arXiv:1407.8150 [hep-ex]].

[10] C. Vafa and E. Witten, "Restrictions on symmetry breaking in vector-like gauge theories," Nucl. Phys. B **234**, 173 (1984).

[11] See, e.g., S. Weinberg, *The Quantum Theory of Fields Volume II*, (Cambridge University Press, Cambridge, United Kingdom, 1996).

[12] G. Aad *et al.* [ATLAS Collaboration], "Searches for heavy long-lived charged particles with the ATLAS detector in proton-proton collisions at $\sqrt{s} = 8$ TeV," JHEP **01**, 068 (2015) [arXiv:1411.6795 [hep-ex]]; S. Chatrchyan *et al.* [CMS Collaboration], "Searches for long-lived charged particles in pp collisions at $\sqrt{s} = 7$ and 8 TeV," JHEP **07**, 122 (2013) [arXiv:1305.0491 [hep-ex]].

[13] H. Georgi and S. L. Glashow, "Unity of all elementary particle forces," Phys. Rev. Lett. **32**, 438 (1974).

[14] J. A. Aguilar-Saavedra, R. Benbrik, S. Heinemeyer and M. Pérez-Victoria, "Handbook of vectorlike quarks: mixing and single production," Phys. Rev. D **88**, 094010 (2013) [arXiv:1306.0572 [hep-ph]].

[15] L. J. Hall and Y. Nomura, "A finely-predicted Higgs boson mass from a finely-tuned weak scale," JHEP **03**, 076 (2010) [arXiv:0910.2235 [hep-ph]].

[16] C. Kilic, T. Okui and R. Sundrum, "Vectorlike confinement at the LHC," JHEP **02**, 018 (2010) [arXiv:0906.0577 [hep-ph]]; C. Kilic and T. Okui, "The LHC phenomenology of vectorlike confinement," JHEP **04**, 128 (2010) [arXiv:1001.4526 [hep-ph]].

[17] ATLAS collaboration, "Search for WW, WZ, and ZZ resonances in pp collisions at $\sqrt{s} = 8$ TeV with the ATLAS detector," ATLAS-CONF-2015-045.

[18] G. Aad *et al.* [ATLAS Collaboration], "Search for new phenomena in the dijet mass distribution using p-p collision data at $\sqrt{s} = 8$ TeV with the ATLAS detector," Phys. Rev. D **91**, 052007 (2015) [arXiv:1407.1376 [hep-ex]].